ELSEVIER

Clinical Radiology (2003) **58**: 1–19
doi:10.1053/crad.2003.1157, available online at www.sciencedirect.com

Review

Magnetic Resonance Imaging of Short T_2 Components in Tissue

P. D. GATEHOUSE*, G. M. BYDDER*†

**The Cardiac Magnetic Resonance Unit, Royal Brompton Hospital, London, U.K.*
and †The Robert Steiner Magnetic Resonance Unit, Imaging Sciences Department, MRC Clinical Sciences Centre, Imperial College Faculty of Medicine, Hammersmith Hospital, London, U.K.

Received: 27 September 2002 Revised: 18 October 2002 Accepted: 18 October 2002

The most widely used clinical magnetic resonance imaging techniques for the diagnosis of parenchymal disease employ heavily T_2-weighted sequences to detect an increase or decrease in the signal from long T_2 components in tissue. Tissues also contain short T_2 components that are not detected or only poorly detected with conventional sequences. These components are the majority species in tendons, ligaments, menisci, periosteum, cortical bone and other related tissues, and the minority in many other tissues that have predominantly long T_2 components.

The development and clinical application of techniques to detect short T_2 components are just beginning. Such techniques include magic angle imaging, as well as short echo time (TE), and ultrashort TE (Ute) pulse sequences. Magic angle imaging increases the T_2 of highly ordered, collagen-rich tissues such as tendons and ligaments so signal can be detected from them with conventional pulse sequences. Ute sequences detect short T_2 components before they have decayed, both in tissues with a majority of short T_2 components and those with a minority. In the latter case steps usually need to be taken to suppress the signal from the majority of long T_2 components. Fat suppression of different types may also be helpful. Once signal from short T_2 components has been detected, different pulse sequences can be used to determine increases or decreases in T_1 and T_2 and study contrast enhancement.

Using these approaches, signals have been detected from normal tissues with a majority of short T_2 components such as tendons, ligaments, menisci, periosteum, cortical bone, dentine and enamel (the latter four tissues for the first time) as well as from the other tissues in which short T_2 components are a minority. Some diseases such as chronic fibrosis, gliosis, haemorrhage and calcification may increase the signal from short T_2 components while others such as loss of tissue, loss of order in tissue and an increase in water content may decrease them. Changes of these types have been demonstrated in tendonopathy, intervertebral disc disease, ligament injury, haemachromatosis, pituitary perivascular fibrosis, gliomas, multiple sclerosis and angiomas.

Use of these techniques has reduced the limit of clinical detectability of short T_2 components by about two orders of magnitude from about 10 ms to about 100 μs. As a consequence it is now possible to study tissues that have a majority of short T_2 components with both "bright" and "dark" approaches, with the bright (high signal) approach offering options for developing tissue contrast of different types, as well as the potential for tissue characterization. In addition, tissues with a minority of short T_2 components may demonstrate changes in disease that are not apparent with conventional heavily T_2-weighted sequences. Gatehouse, P. D. and Bydder, G. M. (2003). *Clinical Radiology* **58**, 1–19.

Key words: magnetic resonance imaging, short T_2 components, ultrashort echo times.

Author for correspondence: Dr G. M. Bydder, The Robert Steiner Magnetic Resonance Unit, Hammersmith Hospital, Du Cane Road, London W12 0HS, U.K. Tel: +44-20-8383-3298; Fax: +44-20-8383-3038; E-mail: graeme.bydder@csc.mrc.ac.uk Guarantors of study: Drs P. D. Gatehouse and G. M. Bydder.

INTRODUCTION

The most common method for diagnosing parenchymal disease in clinical magnetic resonance (MR) imaging involves

0009-9260/03/$30.00/0

the use of heavily T_2-weighted sequences to detect an increase or decrease in long T_2 components in tissue. This approach has been successful for over 20 years, and encompasses conventional spin-echo sequences, as well as newer developments such as fast spin-echo imaging, fluid attenuated inversion recovery (FLAIR), clinical EPI, diffusion-weighted imaging and susceptibility weighted imaging (Fig. 1).

In addition to long T_2 components, tissues contain short T_2 components. In some tissues such as tendons, ligaments, menisci and cortical bone these are the majority species. Conventional clinical methods are insensitive to these components, and so these tissues typically have a low or zero signal intensity with all pulse sequences (Fig. 2*a*). They include tissues that are virtually always of zero signal intensity (e.g. periosteum, cortical bone, dentine, enamel) and others in which a signal may be detectable depending on the pulse sequence used (e.g. meninges, falx) (Table 1). The lack of signal is useful diagnostically to provide a dark background against which high- signal abnormalities can be recognized, but it has meant that the options for developing tissue contrast of different types have been limited, and that these tissues have been poorly characterized in MR terms because there has been little or no signal available to manipulate with different pulse sequences.

Other tissues besides tendons, ligaments and related tissues contain short T_2 components but as a minority species (Fig. 2*b*). These components typically arise from protons in water closely associated with macromolecules (or protons actually within macromolecules) in cell membranes and intracellular structures, and are found to some extent in all tissues. Signals from these sources are not usually detected, or poorly detected with conventional pulse sequences.

To place these observations in a quantitative context, it has generally been thought that conventional clinical MR imaging does not detect signals from tissues with T_2s less than 10 ms [1]. Protons in water associated with macromolecules have T_2s less than 1 ms and protons in water very closely associated with macromolecules, or actually within macromolecules, have T_2s of about 10 μs [1].

Although those working in solid-state imaging are familiar with the problems of detecting signals from materials with a very short T_2s, there has been little clinical work performed in this area. Over the last decade less than 20 patients have been reported using techniques that specifically detect short T_2 components, and no patient studies have been described in major areas of clinical interest such as the brain, liver, pelvis and spine.

This paper describes approaches to detecting and characterizing short T_2 components in tissues for clinical purposes.

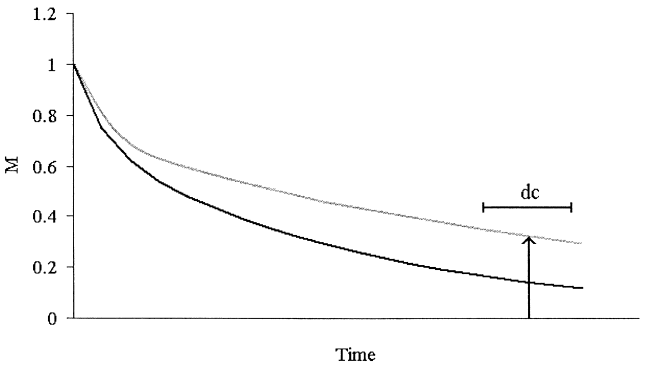

Fig. 1 – T_2 dependent decay of tissue magnetization and detection of long T_2 components. The decay for a normal tissue is shown in the lower curve and that for a tissue with an increased T_2 in the upper curve. The data collection (dc) is shown. The signal intensity in a voxel is proportional to the height of the signal during the data collection (vertical arrow) at the echo time (TE). A higher signal than in normal tissue is present in the abnormal tissue during the data collection which is obtained with a long TE.

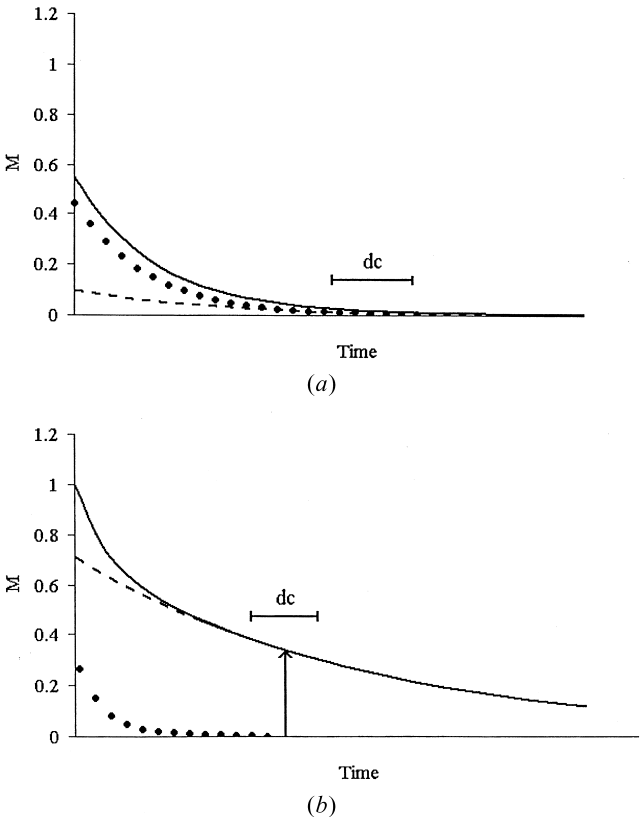

Fig. 2 – Magnetization decay (solid line) in a tissue with a majority of short T_2 components. The circles represent the short T_2 components which decay rapidly. In (a) the long T_2 components (dashed lines) are present in a much lower concentration and decay more slowly. At the data collection (dc) with an intermediate TE there is little or no signal. Magnetization decay (solid line) in a tissue with a minority of short T_2 components is shown in (b). The short T_2 components (circles) decay rapidly and give no signal. The detected signal comes from the long T_2 components (dashed line).

Table 1 – Tissues with a majority of short T_2 components

Short and very short T_2s (usually zero signal with conventional pulse sequences)	Moderately short T_2s (usually zero or low signal with conventional pulse sequences)
Tendons (most)	Retinaculi (some)
Ligaments (most)	Fasciae (some)
Menisci	Bands (some)
Labri	Septa (some)
Periosteum	Membranes (some)
Cortical bone	Capsules (some)
Dentine	Meninges
Enamel	Falx

MAGIC ANGLE IMAGING

The observation that the MR signal from collagen shows a directional dependence was first made by Berensden in 1962 [2]. This is due to dipolar interactions between protons in water, which are tightly bound to highly ordered collagen. The MR signal typically shows a dependence on the term $(3\cos^2\theta - 1)$ where θ is the orientation of the collagen fibres to the static magnetic field Bo. When $\theta = 55°$ (approx.), $3\cos^2\theta - 1 = 0$ and dipolar interactions are minimized. Fullerton *et al.* [3], Peto *et al.* [4], Koblik *et al.* [5] and Henkelman *et al.* [6] have studied *in vitro* tendon samples and shown that the T_2s of tendon samples when their orientation is increased from 0° to 55°, as would be expected from a reduction in dipolar interactions. Henkelman *et al.*, reported that the mean T_2 of *in vitro* dog Achilles tendon increased from 7 to 23 ms when the orientation was changed from 0° to 55°, most of the increase came from the short T_2 components. The T_1 increased only slightly [6].

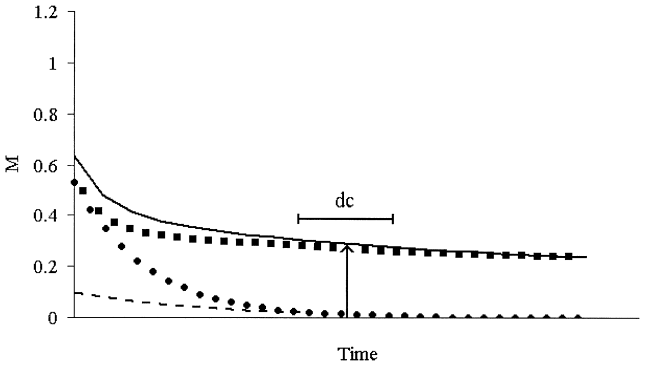

Fig. 3 – Magic angle imaging in a tissue with a majority of short T_2 components. The short T_2 components in the tissue at the magic angle have their normal T_2s (circles) prolonged (squares) and decay much more slowly, so that signal is detectable from them during the data collection (dc).

Although Fullerton *et al.*, suggested that the magic angle effect could be used to make collagen-rich materials more visible on MR images in 1985 [3], this effect subsequently gained clinical attention as a source of unwanted artefact in tendons, ligaments and the posterior horn of the lateral meniscus when all or part of these structures happened to be orientated at 55° to Bo [7,8]. It is only recently that the magic angle effect has been deliberately used as a technique for clinical imaging [9,10]. This type of imaging is illustrated in principle in Fig. 3 and in practice in Fig. 4 where no signal is seen in the Achilles tendon at 0° using an echo time (TE) of 4.8 ms gradient echo sequence and high signal is seen using the same sequence at 55°. Magic angle imaging has been used to visualize contrast enhancement and identify abnormalities after injury [9,10]. Contrast enhancement may be very obvious with the tendon at 55° when it is not detectable at 0° (Fig. 5).

The main advantages of magic angle imaging are that it is easy to perform and can be effective with a wide range of pulse sequences for tendons and ligaments (e.g. from a TE of 40 ms down). The difference in signal with orientation is relatively specific. The main disadvantages are that it ideally requires a linear orientation of the collagen-rich fibres and some positions are not achievable for practical reasons. As a result it has a limited range of clinical application.

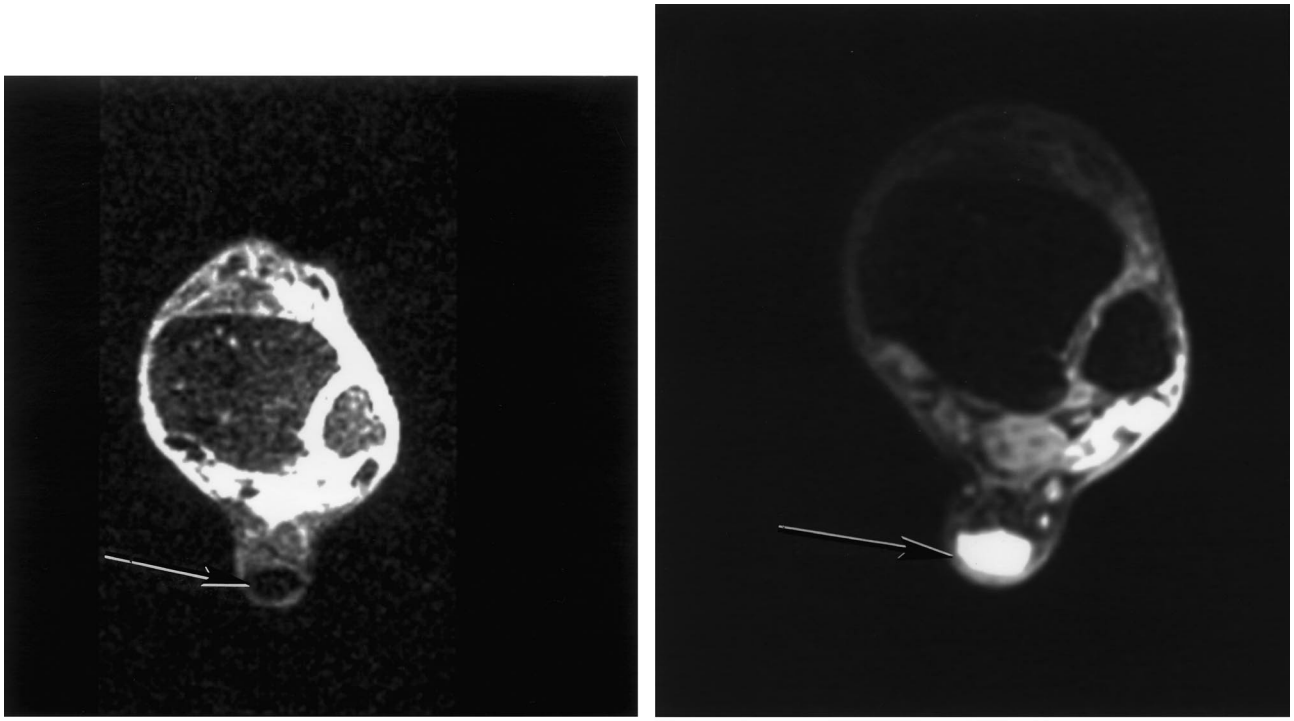

(*a*) (*b*)

Fig. 4 – Normal Achilles tendon at 0° and 55°. Transverse gradient echo 500/4.8 images at 0° (*a*) and 55° (*b*). There is marked increase in the signal from the Achilles tendon (arrows) when it is placed at 55°.

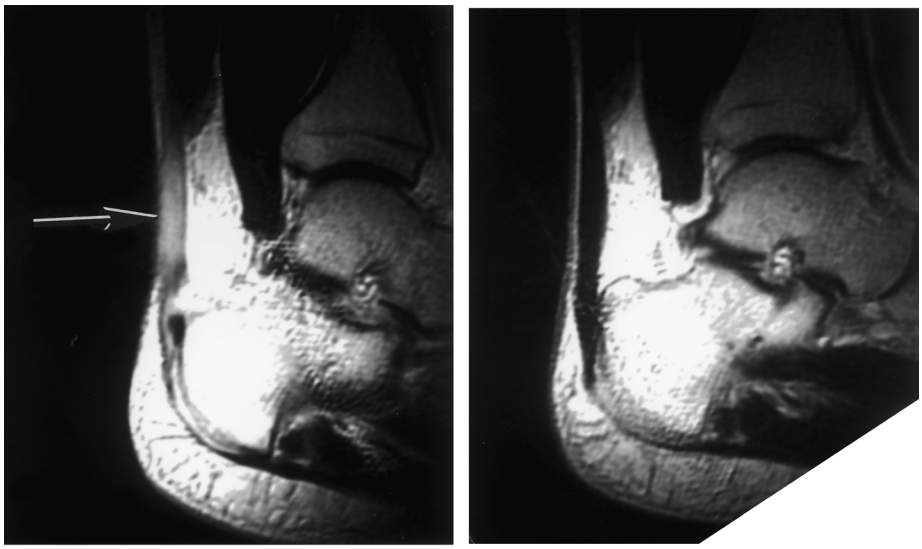

(*a*) (*b*)

Fig. 5 – Chronic Achilles tendonopathy with contrast enhancement. IR 1500/16/300 images obtained at 55° one hour after contrast enhancement (*a*) and at 0° about 5 min later (*b*). The marked contrast enhancement seen on (*a*) at the magic angle (arrow) is not visible with the tendon at 0° on (*b*).

SHORT TE IMAGING (TE = 2–5 MS)

In order to detect the short T_2 components of tendons TE may be shortened so that the signal can be detected before it has decayed. Short TE imaging has been used by Koblik *et al.* [5] and Schick *et al.* [11] with TEs of 3 ms and 4 or 5 ms, respectively. The early studies were on normal equine tendon, and the later ones on small numbers of volunteers and patients. Two out of seven cases of Achilles tendonopathy showed abnormality with short TE sequences which were not seen with conventional longer TE sequences [11].

The main advantage of the technique is that it is readily available. The main disadvantages are that short TE imaging alone may not be sufficient to provide high signal in tendons and ligaments irrespective of their orientation. Short TE imaging is synergistic with magic angle imaging but concurrent use of the two techniques carries with it the disadvantages associated with magic angle imaging.

ULTRASHORT TE (Ute) IMAGING

The term Ute imaging has generally been applied to techniques using unconventional slice selection and radially-acquired projection reconstruction to produce images with very short TEs, typically in the range of 50–250 μs as described by Bergin *et al.*, for lung imaging in 1991 [12], Gold *et al.* [13] and Schmidt *et al.* [14]. The radiofrequency (rf) excitation is performed using a half pulse with the data acquisition beginning at the centre of *k*-space and extending radially. A second rf half pulse excitation is then performed with a reversed slice selection gradient. Each rf pulse is self refocusing, in that no slice rephase gradient is required because $k_z = 0$ is at the end of the slice selection gradient's ramp-down. Combined with the radial centre-out sampling, the TE of central raw data is therefore limited only by how quickly the MR scanner's rf electronics can switch from transmit to receive. Addition of the two signals cancels errors in the two half-rf pulses' slice profiles and produces a single radial line of *k*-space. The process is then repeated through a full range of angles to produce a complete map of two-dimensional (2D) *k*-space. The sequence is a type of gradient echo. All the Ute images in this paper were produced on a Siemens Sonata 1.5 T scanner with off-line reconstruction. First TEs were 80 μs with data sampling intervals of 1–4 μs and typical second and subsequent TEs at 2.87, 5.66 and 8.45 ms (or 5.95, 11.08 and 17.7 ms). The slice thickness was 4–8 mm with 256–1024 excitations. Repetition time (TR) ranged from 10 to 500 ms except for inversion recovery sequences which had TRs of 2200 ms. Flip angles of 30°–80° were used. Breath-hold and cardiac-gated sequences were used. Multislice versions were available for all sequences except the breath-hold and short inversion time variants. Times of acquisition were 12 s to 17 min. Double inversion recovery and FLAIR sequences nulling blood and cerebrospinal fluid (CSF), respectively, were implemented. Intravenous gadodiamide (0.1–0.3 mmol/kg) was administered in selected cases. Permission for these studies was given by the Royal Brompton, Harefield and NHLI Ethics Committee.

Fig. 6 shows the effect of using a Ute sequence in principle, and Fig. 7 is a transverse image of the Achilles tendon in a normal volunteer obtained at 0° with a Ute sequence (TE = 80 μs). Even at an orientation of 0° to Bo, high signal is apparent in the Achilles tendon which has a measured T_2 of about 1.4 ms. High signal is also just apparent in the region of the periosteum of the tibia. It is better seen in the knee images (Fig. 8). Signal has not previously been observed in normal adult periosteum with MR imaging.

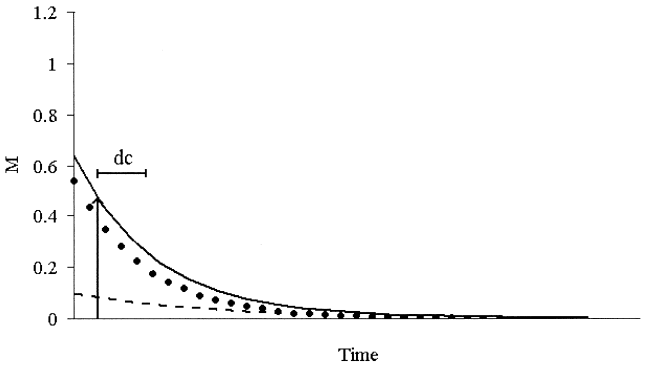

Fig. 6 – Ultrashort TE (Ute) imaging in a tissue with a majority of short T_2 components. The TE is shortened so that signal can be detected before it has decayed. With Ute sequences the effective TE is at the beginning of the data collection (dc).

With Ute techniques the greater signal available at reduced TEs is counterbalanced by the decrease in signal:noise ratio associated with the use of shorter data collections and higher bandwidths. The theoretical optimal data collection duration to maximize signal:noise ratio is of the order of T_2. As a result not just the TE, but the length of data collection of the sequence may need to be optimized for particular values of tissue T_2.

For tissues with a T_2 so short that significant decay occurs during each data collection, isotropic image smoothing is to be expected, because the high spatial frequencies in all directions have been attenuated due to their later acquisition time.

The main advantage of Ute imaging over magic angle imaging is that it is applicable over a full range of angles and positions, and it is effective with complex orientations of fibres and in a wide range of tissues. Ute imaging also minimizes susceptibility artefacts, and water and fat signals do not significantly dephase as they may do with short TE imaging. Ute techniques can be used with preceding preparation pulses, e.g. fat suppression, inversion pulses and long T_2 component suppression (see below).

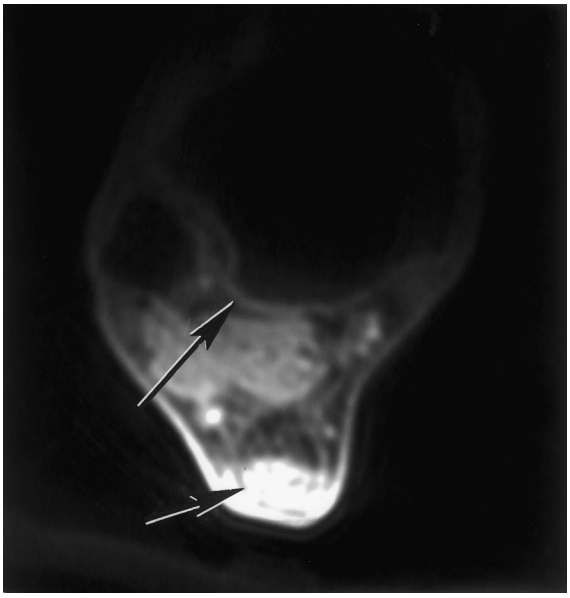

Fig. 7 – Transverse fat-suppressed Ute (Fute) (TR/TE = 500/0.08 ms) images of the Achilles tendon. The tendon has a high signal at 0° (small arrow). Periosteum of the lower end of the tibia at some distance from the surface coil is just visible (large arrow).

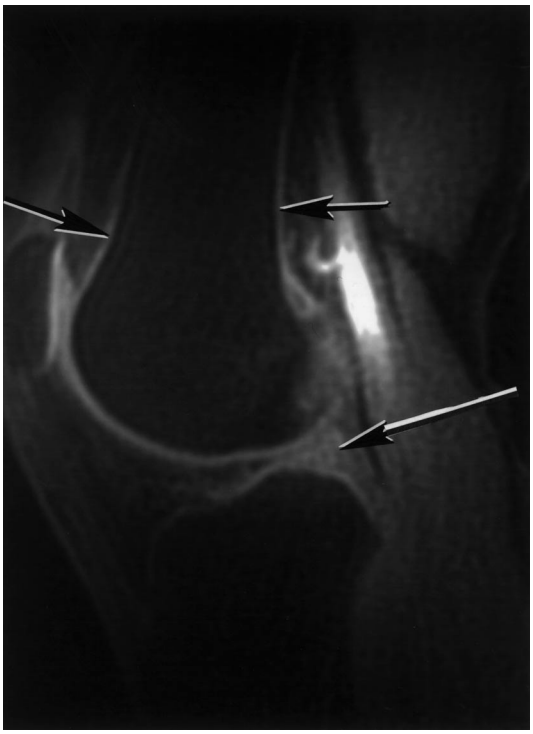

Fig. 8 – Normal periosteum of the knee. Fat suppressed Ute (Fute) (TR/TE = 500/0.08 msec) sagittal image of the knee. The normal periosteum is seen as a high signal structure (short arrows) separate from the cortex. The meniscus (large arrow) has a high signal.

LONG T_2 COMPONENT SUPPRESSION

With tissues containing only a minority of short T_2 components it is often necessary to suppress the long T_2 components in order to isolate the signal from the short T_2 components and thus demonstrate change in disease (Fig. 9). This may also be a useful technique for increasing conspicuity of short T_2 components in relation to other normal and abnormal tissues. To date three main methods have been used to do this.

The first is a long rectangular 90° rf pulse followed by the application of gradients to dephase the signal [15]. With long pulses there is a competition between the rf pulse deviating the magnetization towards the chosen flip angle and T_2 relaxation tending to destroy the magnetizations transverse component, leaving the remaining magnetization subject to longitudinal recovery parallel to Bo. Tissues with a long T_2 have their magnetization nutated or flipped through 90°, but for tissues that have a very short T_2, rapid relaxation is the dominant effect and their magnetization effectively remains orientated along Bo. The overall result is to apply a soft-edged filter to the T_2 components depending on the length of the rectangular pulse. With a 10 ms pulse for example, the magnetization of tissues with a long T_2 of 100 ms or above is flipped through 90°

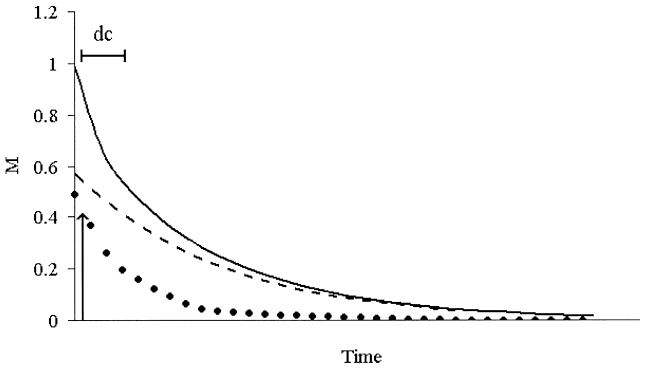

Fig. 9 – Long T_2 suppression with ultrashort TE (Ute) imaging. Techniques are used to reduce the long T_2 components (dashed line) so that the signal from the short T_2 components (circles) can be selectively detected.

(and then dephased) and thus suppressed, while that of tissues with a short T_2 of 1 ms (or less) are essentially unaffected (Fig. 10). The technique requires that the pulse be on-resonance for protons in water, and susceptibility errors may occur from long rf pulses which have a narrow bandwidth. It has the advantage that no further images or image calculations are required but the disadvantage that no source images are available prior to long T_2 suppression.

The second method is to use a long (l) initial inversion pulse to selectively null the long T_2 components. With such a l STIR Ute [or lStute, inversion time (TI) typically <400 ms] sequence (see Table 2) the short T_2 components are effectively transparent to the initial inversion pulse and so experience a "proton density" like sequence, while the long T_2 components are inverted and then can be nulled by the appropriate choice of TI. Note that the length of TI is matched to null the signal that was inverted, whereas the length of the inversion rf pulse itself affects what gets inverted. The effectiveness of the technique is dependent on having a single value of T_1 for the long T_2 components. Comparison with images produced by a short (s) initial inversion pulse which inverts both the short and long T_2 components is helpful (Fig. 11). The main difficulty is that the TI for suppression of long T_2 components may be quite specific and change with disease. If the TI is inappropriate the suppression may be incomplete and so the minority short T_2 components may not be obvious.

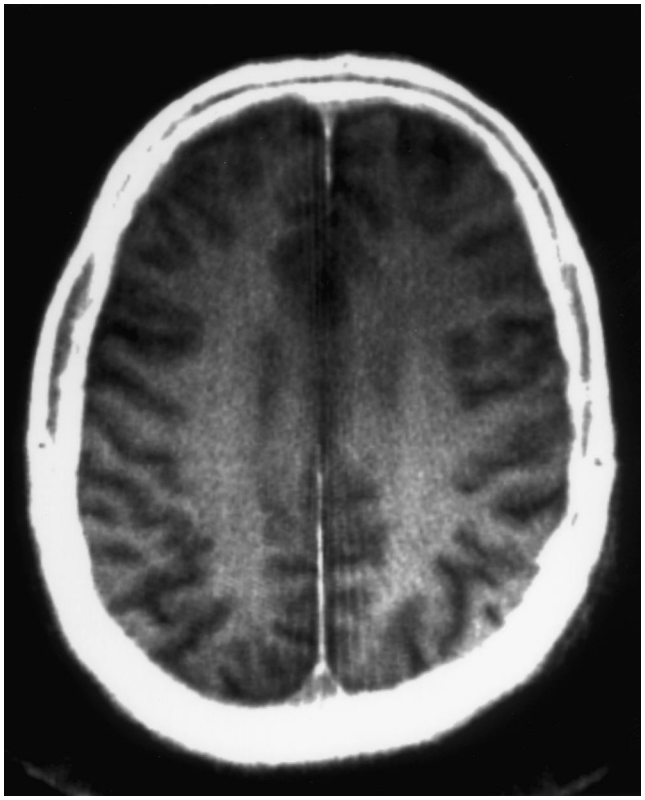

Fig. 10 – Normal brain with long T_2 suppression Lute image (TR/TE = 500/0.08 ms). The general signal level is low because of the low relative concentration of short T_2 components. White matter shows a higher signal than the grey matter.

Table 2 – Ultrashort echo time (Ute) pulse sequences

Conventional Ute	Cute
Long T_2-suppressed Ute (rectangular 90° preparation pulse)	Lute
Fat suppressed (frequency based)	Fute
Fat suppressed (frequency based) and long T_2-suppressed Ute	Flute
Short TI inversion recovery with Ute and long or short initial inversion pulse	l Stute or s Stute
Medium TI inversion recovery with Ute and long or short initial inversion pulse	l Mute or s Mute
FLAIR sequence with Ute	Flaute
Double inversion recovery with Ute	Dute

FLAIR, fluid attenuated inversion recovery; TI, inversion time; STIR, short T_2 inversion recovery.

The third method is by subtraction in the form of a difference (d) image [16]. The signal obtained from a later echo is subtracted from the first echo (or an earlier one) (Fig. 12). This provides a sharper discrimination of short T_2 tissues than the technique using a 90° rectangular pulse followed by dephasing at the expense of increased noise on the image. The subtraction method also has the advantage that the source images are available and can be checked, but second (or later) echoes may introduce susceptibility artefacts.

Normal tissue or material with a high concentration of short T_2 components (e.g. plastic covers of transmit and receive coils, tendons and ligaments, faecal material in the colon and rectum) within the image is useful clinically so that the effectiveness of the detection of short T_2 components with or without suppression of long T_2 components can be monitored.

FAT SUPPRESSION

Different methods of fat suppression have been in clinical use for at least 15 years. Out-of-phase imaging (e.g. gradient echo imaging at TE = 2.2 ms at 1.5 T) may produce cancellation at water–fat boundaries, which may result in a net overall reduction in background signal. This may increase the conspicuity of tissues such as tendons and ligaments when they have a high signal.

Conventional fat saturation based on frequency differences with protons in water is more effective at higher fields (e.g. 1.5 T) but is subject to the problems of shimming and local susceptibility effects at bone–tissue and air–tissue

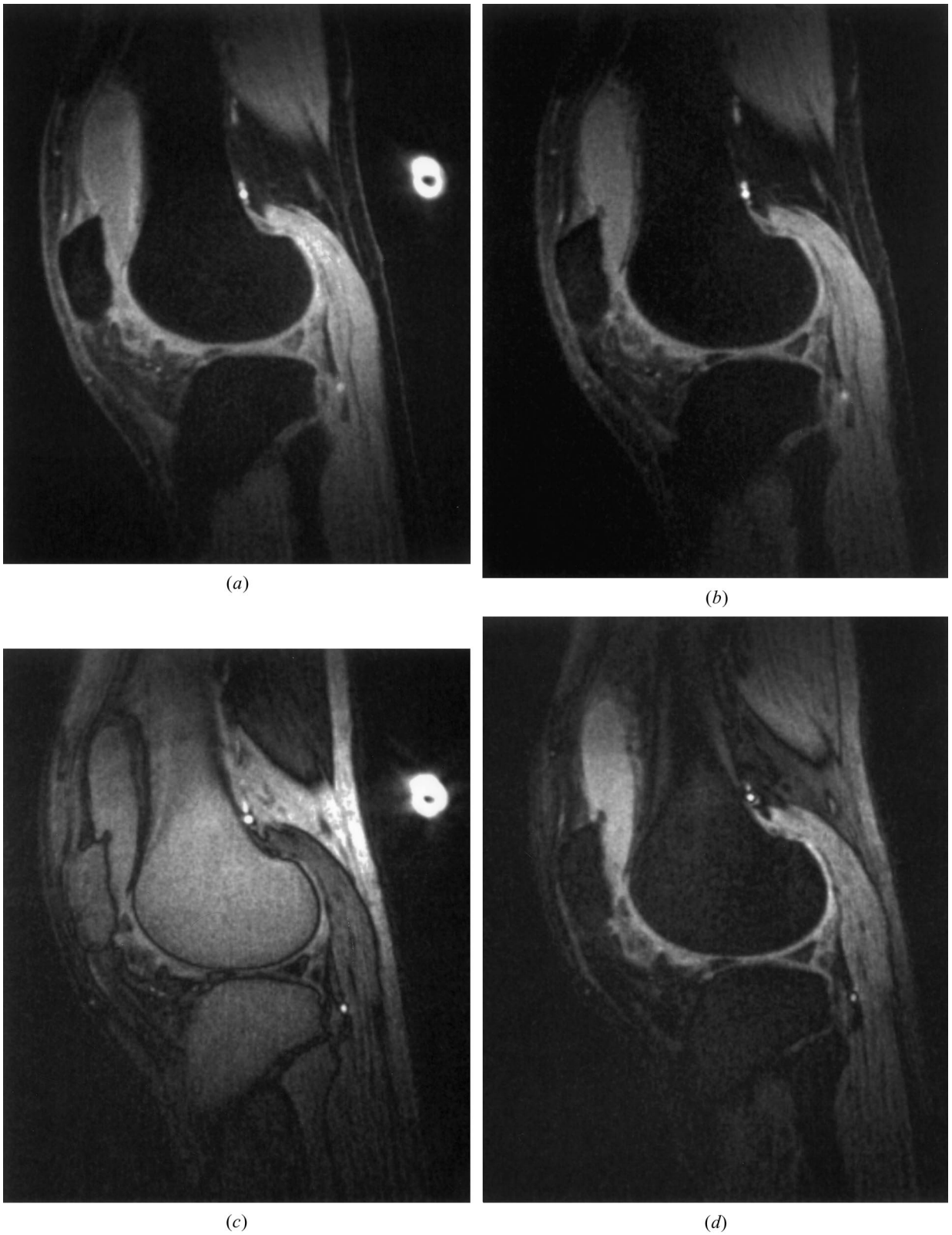

(*a*) (*b*)

(*c*) (*d*)

Fig. 11 – Knee in a patient with chronic arthritis with short and long inversion pulses and nulling of long T_2 components using sagittal s Stute and l Stute (both TR/TE/TI = 2200/0.08/160 ms) sequences. With the short (500 μs) inversion pulse s Stute sequence, fat is nulled at TEs of 0.08 ms (*a*) and 5.95 ms (*b*). With the long (10 ms) inversion pulse l Stute sequence (*c*), the short T_2 components of fat are not nulled and signal is seen in the bone marrow, subcutaneous fat and fat between muscles at a TE of 0.08 ms. The signal from fat is considerably decreased in the later echo of the l Stute sequence at 4.18 ms (*d*) showing that it is coming from tissue with a short T_2. The high signal circular area posterior to the knee on figures (*a*) and (*c*) is from the plastic cover of the circular receiver coil.

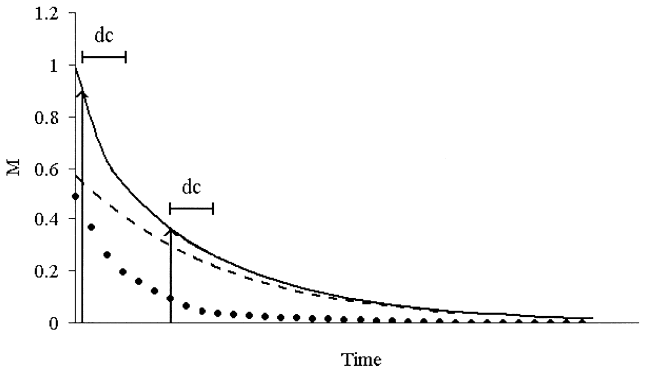

Fig. 12 – Subtraction with ultrashort TE imaging in a tissue with a minority of short T_2 components. Signals are detected at a ultrashort TE and at a later TE. The second signal is subtracted from the first. Most of the difference is due to the reduction in the signal from the short T_2 components.

boundaries. It is also possible that off-resonance fat saturation pulses may saturate the broad lines of short T_2 components and thus reduce the available signal from them. Fat and water selectivity using an oscillating read gradient and the three or four point Dixon technique have been combined with Ute imaging [13] at 1.5 T. At lower static field strengths frequency-based fat saturation is less effective and phase-sensitive techniques such as three point Dixon are usually employed.

The STIR sequence [17] is effective for fat signal suppression, but this may not include the short T_2 components within fat when conventional (relatively long) inversion pulses are used. More complex forms of spectroscopic imaging have been implemented recently [18]. In spite of the difficulties, the effect of fat suppression may be dramatic. Tendons, ligaments, menisci, periosteum and cortical bone may become among the highest signal structures on the image. A fat-suppressed magic angle short TE image of the patellar tendon is shown in Fig. 13.

CONTRAST ENHANCEMENT

There has been relatively little use of intravenous gadolinium chelates in tendon and ligament studies although some authors have reported this method as the most effective technique for the diagnosis of tendonopathy [19]. With conventional imaging techniques contrast enhancement is only detectable in tendons and ligaments in regions which have abnormally increased T_2s. When imaged at the magic angle however, change in signal is detectable in the normal tendon. The enhancement typically has a long time course. In addition abnormal enhancement may only be apparent when the tendon or ligament is imaged at the magic angle [10], and see Fig. 5.

An inversion recovery pulse sequence with TI chosen to allow signal recovery just beyond the null point (i.e. a medium TI sequence) is valuable in magic angle imaging. This provides a relatively uniform low signal for the tendon or ligament (defined by its T_1) but high sensitivity to contrast enhancement by virtue of the use of a highly T_1 dependent form of inversion recovery sequence and the fact that the T_2 of the tendon is increased by the magic angle effect (see Fig. 5).

Ute sequences are also valuable for showing contrast enhancement for tissues with a majority of short T_2 components as they provide a mechanism for detecting signal which may change as a result of gadolinium chelates shortening T_1. It is notable that the signal produced by contrast enhancement decreases rapidly with increasing TE (e.g. 0.08, 5.95 ms in Fig. 14). This may be due to susceptibility effects becoming obvious at shorter TEs than was previously suspected.

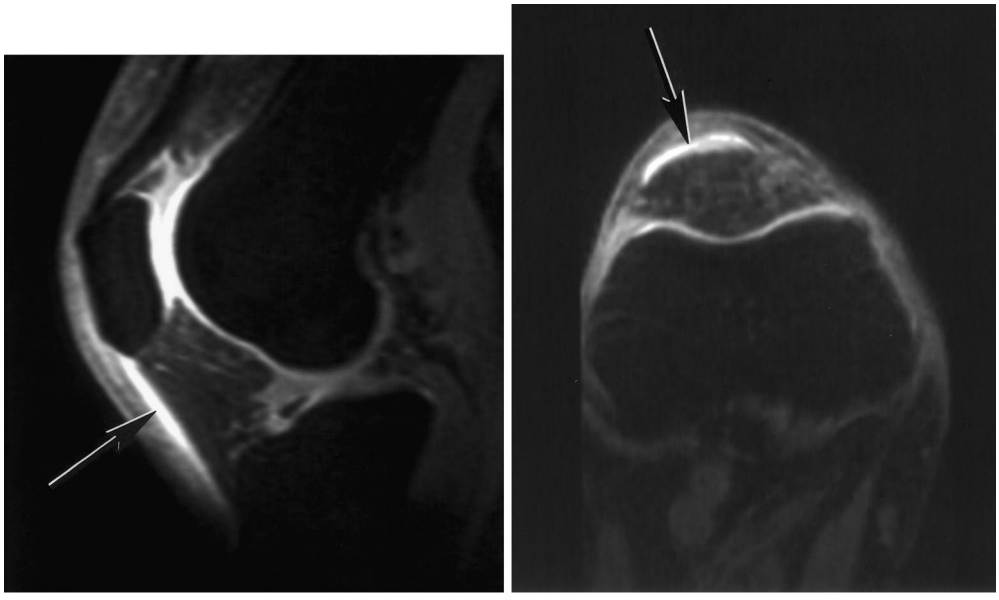

(*a*) (*b*)

Fig. 13 – Fat-suppressed gradient echo of the patellar tendon (TR/TE = 300/4.2 ms). Sagittal (*a*) and transverse (*b*) magic angle images of the patellar tendon. The tendon (arrows) has a high signal against the muted background of muscle, fat and other tissues (except articular cartilage).

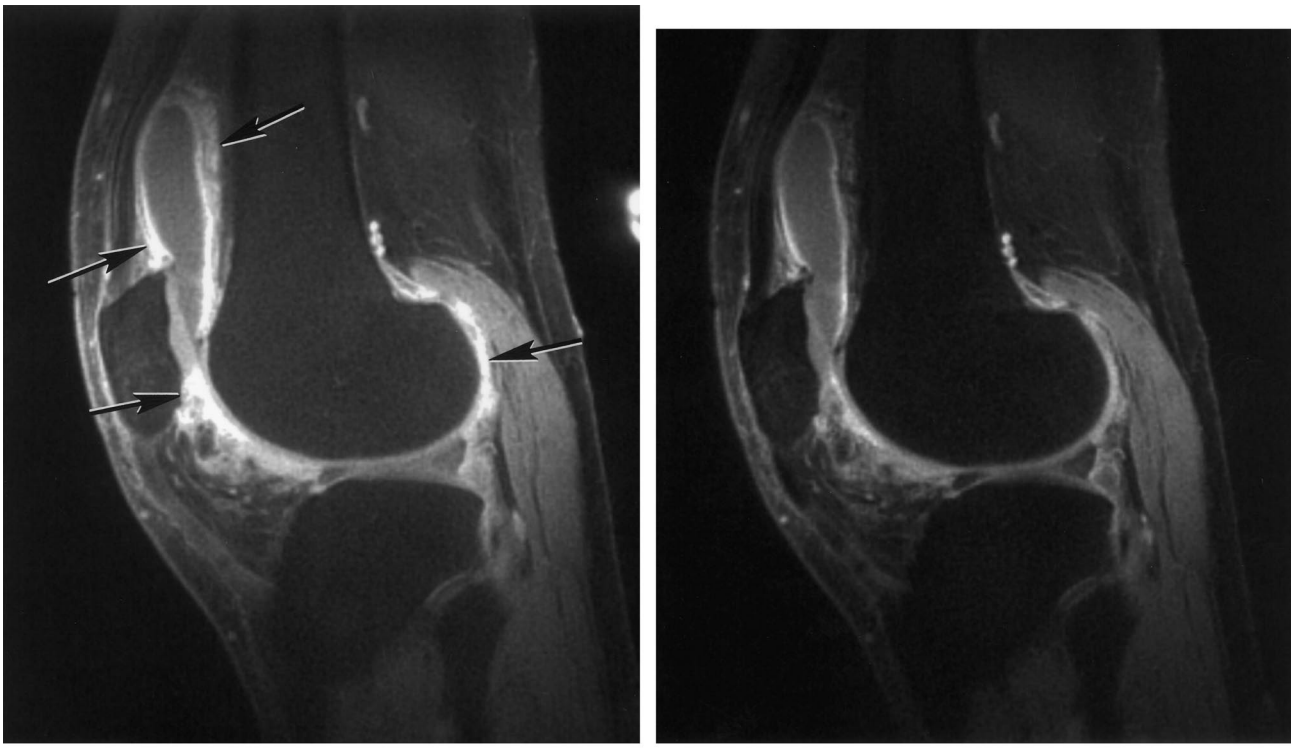

(*a*) (*b*)

Fig. 14 – Sagittal knee Fute images. (TR/TE = 500/0.08 ms, *a*) and (TR/TE = 500/4.18 ms, *b*) after intravenous gadolinium DTPA in a patient with chronic arthritis. Enhancement of the synovium is more obvious on the early echo in (*a*) (arrows) than on (*b*) which was obtained simultaneously.

Magnetic iron oxide particles would also be of interest. In tissues with a minority of short T_2 components, they may shorten the T_2 of the long T_2 components and increase the detectable signal from short T_2 components and produce different conspicuity options.

MAGNETIZATION TRANSFER

The relationship between imaging of short T_2 components and magnetization transfer imaging is of considerable interest [1,20]. Both approaches are concerned with deriving information about short T_2 components. Ute imaging does this directly, and magnetization transfer does this indirectly by saturating the short T_2 components in the bound pool and determining what effect this has on the detectable long T_2 components in the free pool.

In tissues with a majority of short T_2 components magnetization transfer imaging is not possible with conventional approaches as there is effectively no free pool to detect signal from. With magic angle imaging some tissues T_2s are lengthened and so a free pool is created and magnetization transfer effects can then be studied [9].

With both multislice imaging and frequency based fat suppression, off-resonance pulses are applied, and these may saturate short T_2 components (which have a broad line width) and thus reduce the signal detectable with Ute sequences.

Clinical results with conventional MT sequences may provide a guide to applications of Ute sequences in tissues with a minority of short T_2 components. For example, in multiple sclerosis decreased magnetization transfer in white matter may be associated with a reduction in signal from short T_2 components.

ARTEFACTS

The magic angle effect has received most recognition as a source of unwanted artefact in the form of spurious high signals from tendons and ligaments (or parts of them) which happen to be at 55° to Bo. With magic angle imaging, where the objective is to place these structures at 55° to achieve high signals, low signal may be seen as an apparent abnormality if the magic angle is not achieved.

The magic angle effect may be seen in different ways with Ute imaging. With difference images, the signal may not drop as expected on the later echoes so that there is an apparent prolongation of T_2 with an apparent loss of short T_2 components. It may be necessary distinguish to this from disease.

With the Ute, imaging projection reconstruction may lead to radial artefacts at the periphery of the image in a way familiar for x-ray CT. As with CT projection reconstruction images, “dishing” or “doming” of images may result in low or higher signal in the centre of the image compared with the periphery.

Another phenomenon is a higher signal on l Stute images in the cortical grey matter of the second echo compared with the first echo, which is not evident in central grey matter. On the differences images obtained from early (0.08 ms) minus later echo images, it is manifest as a negative signal from the

cerebral cortex. This may be due to an overshoot phenomenon adjacent to the high signal from the bone marrow and scalp analogous to the spurious brain "cortex" signal seen on early CT images. Susceptibility artefacts become more obvious with the longer TE images used to produce difference images.

Tissues with a short T_2 compared with the half-rf pulse duration used in the Ute sequences have a broadened slice profile and a reduced effective nutation angle. This effect occurs for the same reason as outlined previously for long T_2 suppression pulses, i.e. transverse relaxation during the rf excitation.

An inherent assumption of the half-rf pulse technique is that errors in the two half pulse profiles will be of opposite phases, so that the errors cancel out when the two are summed, leaving only the desired slice profile. Some caution is necessary when applying these pulses in multislice interleaving and when using them with surface coils where there may be high signals present outside of the desired slice profile.

OTHER TECHNIQUES FOR INCREASING SIGNAL AND PROVIDING A GREATER SPECIFICITY

A branch of MR is concerned with the imaging of solid structures. Unlike the soft tissues of most interest in clinical practice, solids have extremely short T_2s (of the order of microseconds) and long T_1s (which may be minutes or even hours instead of milliseconds). A variety of techniques have been developed to detect signal very early after excitation, or use pulse sequences to rephase rapidly decaying signals.

Magic sandwich echo (MSE) imaging [21] is one such technique in which a multiple 180° pulses are applied (the "sandwich") after the initial 90° pulse and before a gradient or spin echo data collection. The sandwich pulses are designed to rephase the rapidly decaying signal. The technique has been applied to tendon samples *in vitro*, and human volunteers. It has been used in the form of a spin-echo sequence (with and without the additional sandwich pulses). The ratio of the increase in signal with the use of the sandwich pulse to the baseline value without the sandwich gives a measure of the dipolar interactions. This increase was found to be 40% for cartilage, 30% for tendon and 10% for muscle [22].

Another more complex sequence that has been applied in studies of the normal and healing rabbit tendons, ligaments and cartilage, as well as the normal human wrist and ankle, is double quantum filter imaging [23,24]. The technique depends on the presence of dipolar interactions in ordered structures. The available signal is relatively small and the imaging times consequently are relatively long. The technique is not dependent on tissue position and is specific for highly coupled nuclei. Neither magic sandwich echo nor double quantum filter imaging has yet been used in patient studies.

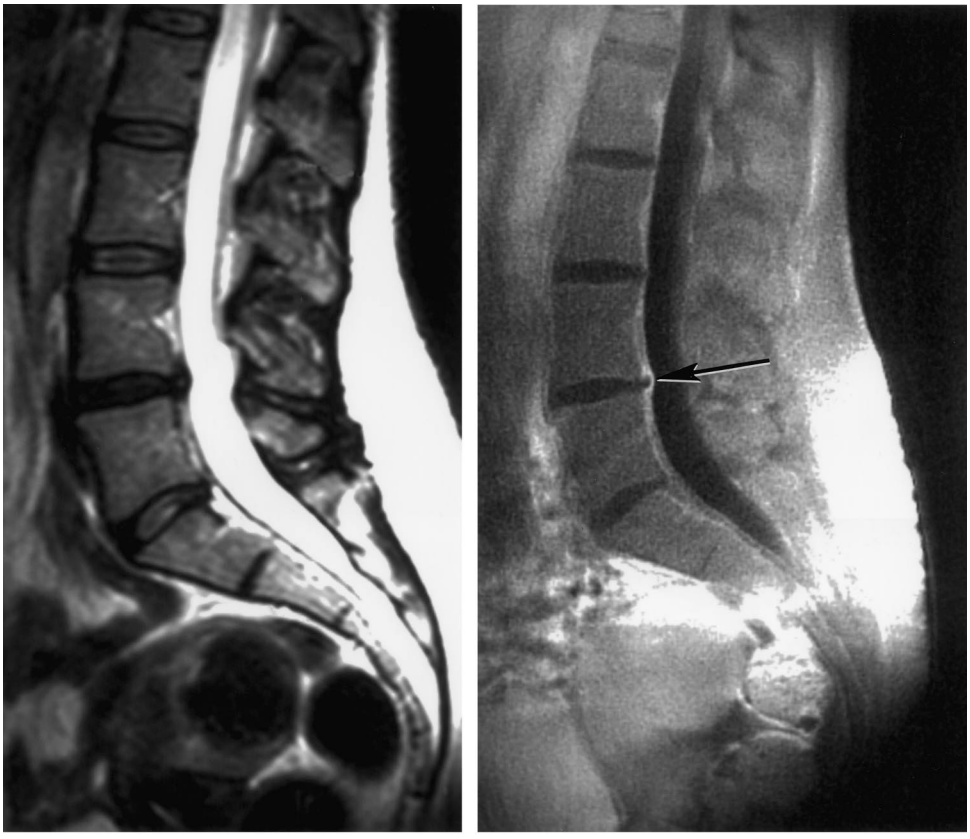

(*a*) (*b*)

Fig. 15 – Sagittal scans of the lumbar spine in a patient with mild disc disease. Sagittal T_2-weighted (TR/TE 2500/90) (*a*) and d Flute (TR/TE = 500/0.08 ms) (*b*) images. The region of the probable scarring opposite the bulging disc has a high signal on (*b*) (arrow). It is not specifically identifiable on (*a*).

CHANGES IN DISEASE

A variety of pathological processes may increase or decrease the signal from short T_2 components. Increases are likely in fibrosis (especially if chronic), gliosis, phases of haemorrhage, calcification and increased iron deposition. Decreases in short T_2 component signals are likely with loss of tissue, loss of order in tissue, demyelination and oedema (with shift of short T_2 components to become long T_2 components).

Where there is no change apparent with conventional long T_2 component approaches, abnormalities may be apparent with short T_2 approaches in situations where spectroscopy or other techniques have suggested disease is present.

In general terms, contrast enhancement has previously only been detectable in tissues such as tendons and ligaments with a majority of short T_2 components in abnormal areas which have an increased T_2 so there is scope to apply contrast agents more widely. In tissues with a minority of short T_2 components, contrast enhancement may differ from that with conventional approaches based on detection of long T_2 components.

EXAMPLES

Examples involving normal and diseased tissues with a majority of short T_2 components followed by those with a minority are illustrated: Fig. 15 shows conventional T_2 weighted (*a*) and Flute (*b*) images in a case of mild disc bulging at L4/L5. At the posterior aspect of the disc there is a high signal intensity region consistent with localized scar formation (*b*). This is not apparent on the conventional T_2 weighted image.

Fig. 16 shows a d Cute image with high signal from the meniscus and two separate layers apparent in articular cartilage. Spectroscopic broad lines associated with deep articular cartilage and narrow lines associated with the superficial layer have previously been shown [25,26]. This image demonstrates the two different layers directly.

Fig. 17 shows sagittal scans of the knee after gadolinium chelate enhancement Fute images in a patient with a 15 month history of a severe skiing injury. High signal is seen in the patellar tendon (arrow) and posterior cruciate ligament (arrow).

A transverse image through the tibia with a d Fute image taken with a surface coil adjacent to the tibia shows high signal from the cortex in Fig. 18. The cortex has a T_2 of about 250 μs [27]. The signal is probably coming from collagen type I and bound water. Signal has not previously been detected from normal cortical bone in volunteers or patients.

The periodontal ligament is seen in Fig. 19*a*. It has not previously been recognized as a separate structure with MR imaging. The difference images show a moderately high signal from dentine and a low signal from enamel (Fig. 19*b*). With an anterior surface coil, high signal is seen from dentine and lower signal is seen from enamel in Fig. 19*c*. The difference image derived from Fig. 19*c* and a later echo shows equal signal levels for dentine and enamel consistent with more rapid decay in signal from the lower signal level in enamel (Fig. 19*d*). *In vitro* studies have shown that dentine has multi-component T_2s with a mean T_2 of about 200 μs [28] and enamel has a mean T_2 of about 60 μs [29] depending on the type of tissue preparation.

The median nerve displays a marked magic angle effect probably as a consequence of its high content of linear collagen fibres (Fig. 20). This effect has not previously been recognized with MR neurography. It is a potential source of confusion if increased signal is regarded as a marker of disease irrespective of tendon orientation to Bo.

High signal is seen in the synovium on the sagittal Fute images in chronic arthritis. This is probably due to chronic fibrosis with the fibrotic tissue having a short T_2 and relatively short T_1 (Fig. 21).

A very large fibroid has a high signal from short T_2 components and shows a signal greater than the normal uterus (Fig. 22).

In a case of haemachromatosis a uniform high signal in seen in the liver on the first echo (Fig. 23*a*) with marked loss of signal on the second echo at 2.13 ms (Fig. 23*b*).

The pituitary gland is shown in a normal female age 24 years in Fig. 24*a*. As expected, the posterior pituitary has a higher signal than the anterior pituitary on the T_1-weighted Fute

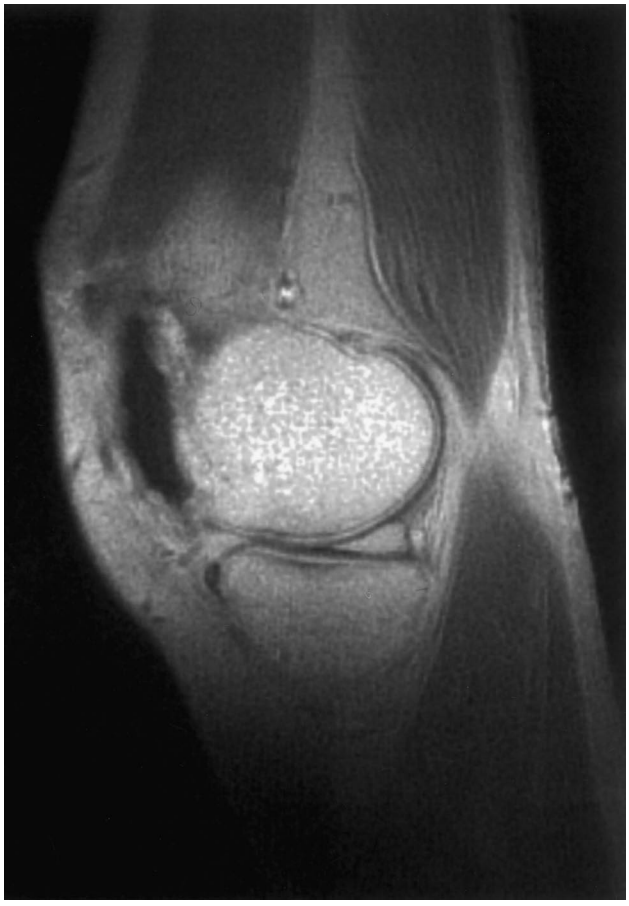

Fig. 16 – Sagittal image of the meniscus and articular cartilage. d Cute (TR/TE = 500/0.08 − TR/TE = 500/5.95 ms). The meniscus has a high signal and the articular cartilage has two layers, a high signal (high short T_2 components) deep layer, and a low signal superficial layer (low short T_2 components and high long T_2 components).

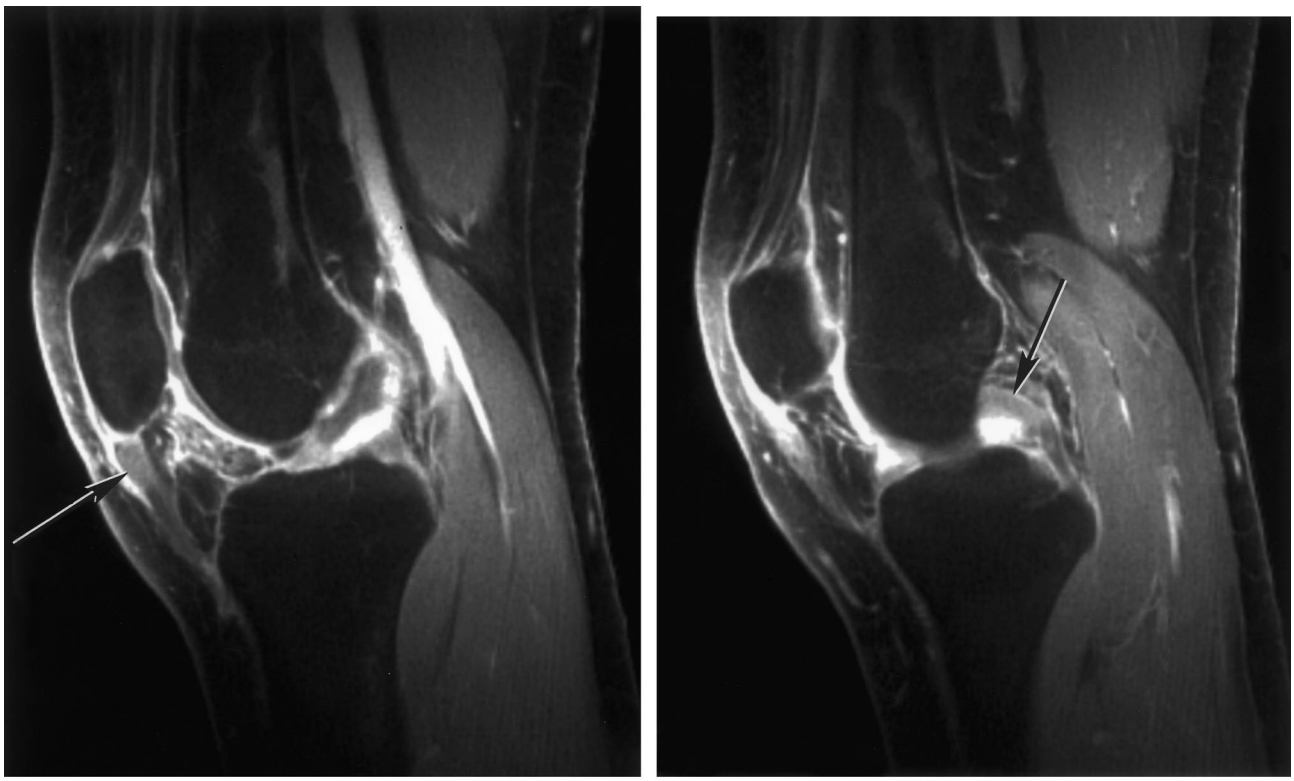

(*a*) (*b*)

Fig. 17 – Sagittal post-enhancement images of the patellar tendon and posterior cruciate ligament. Fute (TR/TE = 500/0.08 ms) images of the knee 18 months after injury. The patellar tendon shows a region of high signal (arrow, *a*) as does the antero–superior aspect of the posterior cruciate ligament (arrow, *b*).

image. In a normal male volunteer aged 58 years examined with the same sequence, high signal is seen in a thick rim around both the anterior and posterior pituitary and the gland is smaller in size. The features are probably due to perivascular fibrosis which is seen with increasing frequency into the tenth decade in post-mortem studies [30]. It is associated with a decrease in somatotrophs. The condition has not previously been recognized with CT or MR imaging.

Fig. 25 is a normal Stute image of the brain obtained from images with TEs of (*a*) 0.08 ms and (*b*) 5.95 ms. The long T_2 components from white matter have been nulled. The difference image (*c*) shows high signal from the normal white matter in the centrum semiovale.

Fig. 26 is from a patient treated for glioma in the left frontal region. There is loss of short T_2 components evident in Fig. 26*b* beyond the region of abnormality shown in Fig. 26*a*.

Fig. 27 is a 46 year old patient 4 years after treatment of a high-grade glioma with surgery, radiotherapy and chemotherapy with a good result. The d Cute (*b*) image shows multiple angiomas (short arrows) which are not apparent on the conventional T_2-weighted image (*a*). (A single large angioma was visible with both conventional and d Cute imaging at a higher level.) The tumour also has a high signal margin probably due to gliosis (long arrow) although this region is isointense on the conventional heavily T_2-weighted image.

Fig. 28 is from a 39 year old woman with a 9 year history of multiple sclerosis. Loss of short T_2 components is apparent in the central white matter. The loss of signal from short T_2 components extends beyond that of many of the lesions seen on the heavily T_2-weighted sequence. Normal short T_2 component signal is only apparent towards the periphery of the hemispheres. In multiple sclerosis a reduction in short T_2 components has been shown in fixed specimens of brain [16,31].

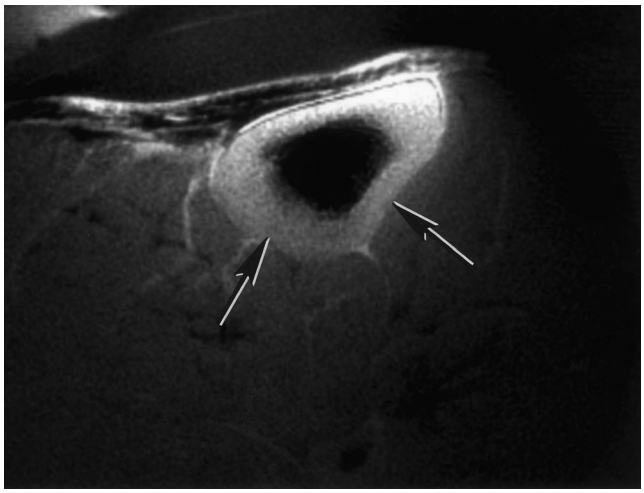

Fig. 18 – Cortex of the tibia. Transverse d Fute (TR/TE = 500/0.08 ms – TR/TE = 500/2.87 ms) image of the normal tibia obtained with a surface coil. Signal is quite obvious in the cortex of the tibia (arrows). It decreases with distance from the surface coil.

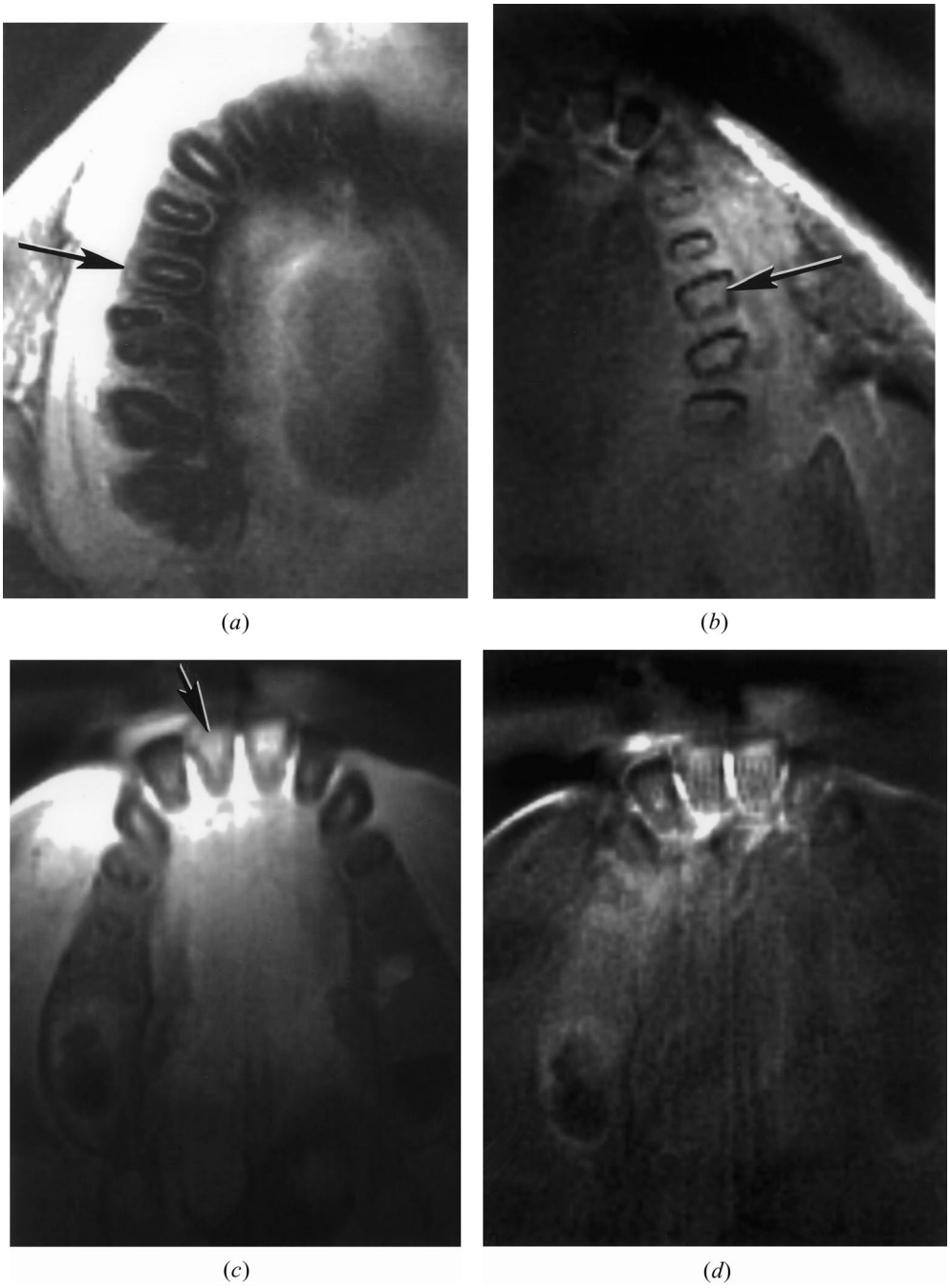

Fig. 19 – Periodontal ligament, dentine and enamel. Transverse Fute (TR/TE = 500/0.08 ms) (*a*), d Fute (TR/TE = 500/0.08 ms − TR/TE = 500/2.87 ms) (*b*), Fute (TR/TE = 500/0.08 ms, (*c*) and d Fute (TR/TE = 500/0.08 and 500/2.87 ms, (*d*). The periodontal ligament is seen on (*a*) (e.g. arrow), dentine is seen on (*b*) (e.g. arrow). Dentine has a higher signal than enamel in the central incisors (arrow on right incisor) in (*c*). On the difference image (*d*) similar levels of signal are seen from dentine and enamel.

DISCUSSION

Use of these techniques has shifted the lower level of detectability of short T_2 components by about two orders of the magnitude from less than 10 ms to less than 100 μs. As a result, by analogy with dark blood and bright blood MR angiography, both "bright" and "dark" approaches are now available to imaging tendons, ligaments, menisci, periosteum, cortical bone and related tissues. The bright, or high-signal approach offers opportunities for different types of conspicuity between normal and abnormal tissues and more specific tissue characterization. For example, the signal available from cortical bone may provide information about collagen and tightly bound water not available with conventional radiological methods based largely

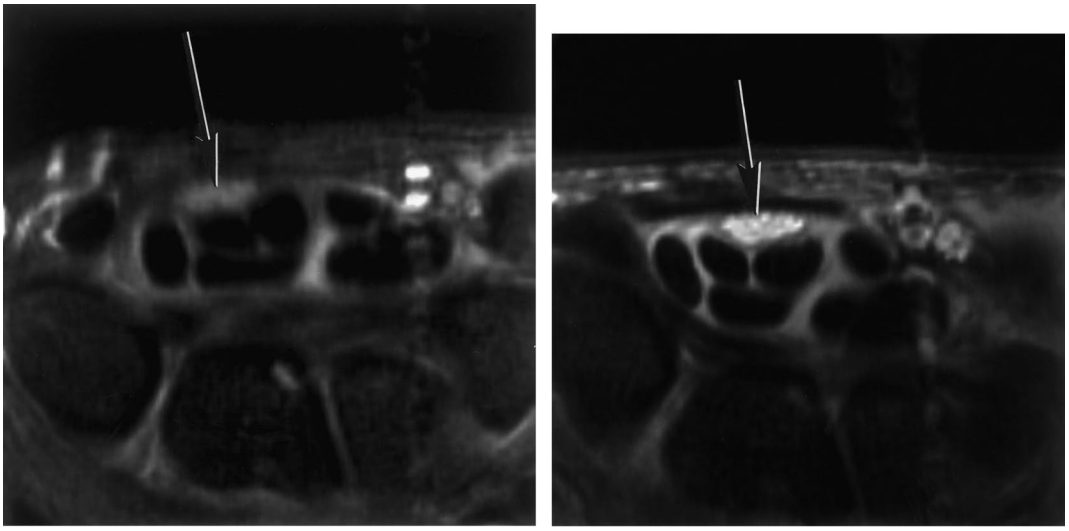

(*a*) (*b*)

Fig. 20 – Magic angle imaging of the median nerve. STIR (TR/TE/TI = 2500/14/160 ms) image at 0° (*a*) and at 55° (*b*). The median nerve has a low signal in (*a*) (arrow) and a high signal with a fascicular pattern in (*b*) (arrow).

on the detection of calcium. In tissues with a majority of short T_2 components evidence of disease may be seen when it is not apparent using conventional approaches based of the detection on long T_2 components.

The techniques described here are in an early phase of development and will need to be optimized for short T_2 component T_1s and T_2s (many of which are not known at the present time) and other factors. In particular, Ute sequences have only been implemented on a very small number of systems. They require somewhat specialized software and there are also specific hardware requirements in terms of gradient performance, as well as rf performance, including rapid

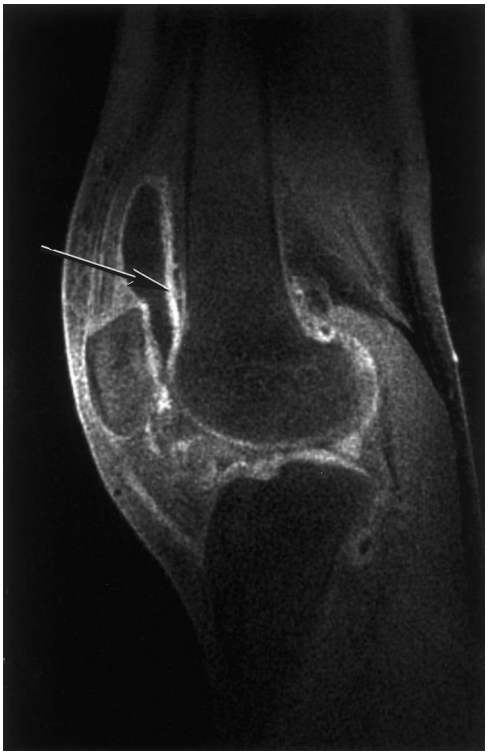

Fig. 21 – Chronic arthritis. Sagittal Fute (TR/TE = 500/0.08 ms) image. High signal is seen in the abnormal synovium (arrow), probably due to fibrosis.

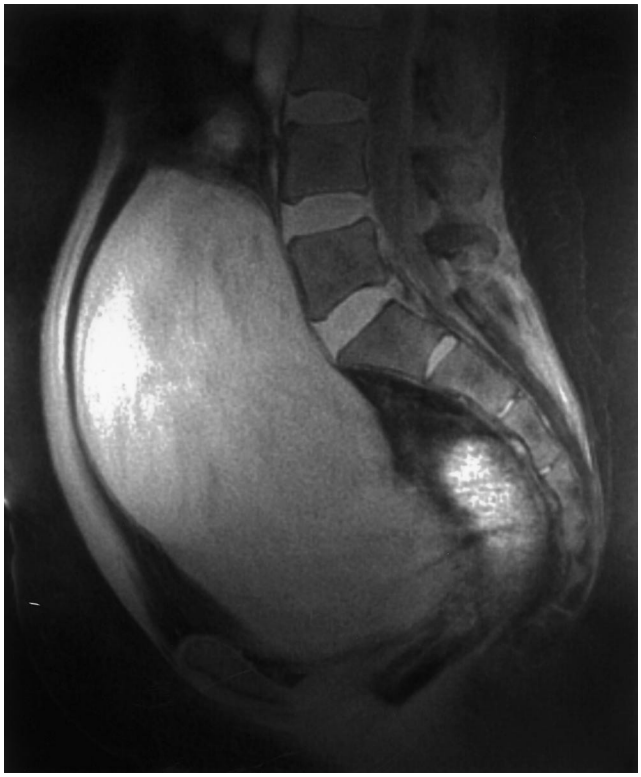

Fig. 22 – Uterine fibroid. Sagittal Fute (TR/TE = 500/0.08 ms) image. The mass has a high signal probably as a consequence of increased fibrous tissue.

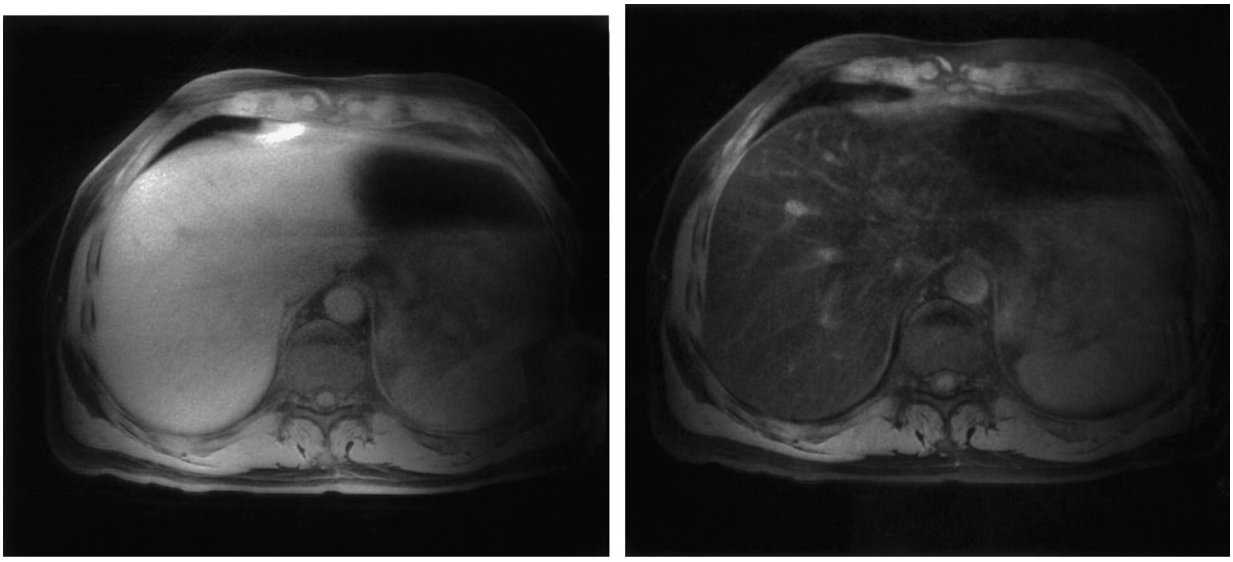

(*a*) (*b*)

Fig. 23 – Haemachromatosis. Transverse Fute images (TR/TE = 500/0.08 ms, *a*) and (TR/TE = 500/2.13 ms, *b*). The liver has a high signal in (*a*) and much lower signal in (*b*).

switching from transmit to receive mode. There is a considerable scope for further development.

In addition, the techniques suffer signal to noise limitations because of the short T_2s in some tissues with a majority of short T_2 components, and the low concentration of short T_2 components (e.g. 2–10%) in other tissues [20]. In spite of these difficulties detection of short T_2 components provides an interesting new approach which may have significant clinical impact.

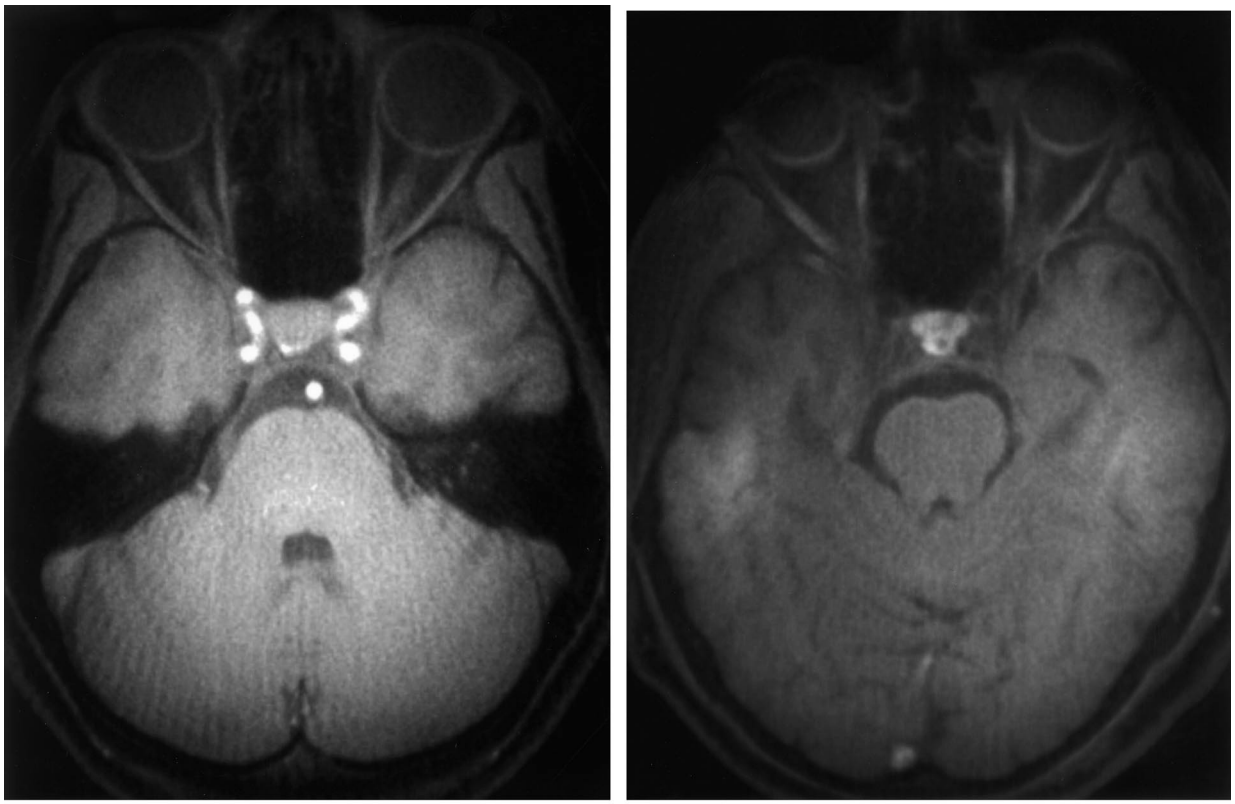

(*a*) (*b*)

Fig. 24 – Pituitary in normal subjects. Transverse Fute (TR/TE = 500/0.08 ms, flip angle 45°) of the pituitary gland in a 24 year old female (*a*) and a 58 year old male (*b*). The posterior pituitary has a high signal in (*a*) but both the anterior and posterior glands show regions of high signal in (*b*) possibly due to perivascular fibrosis.

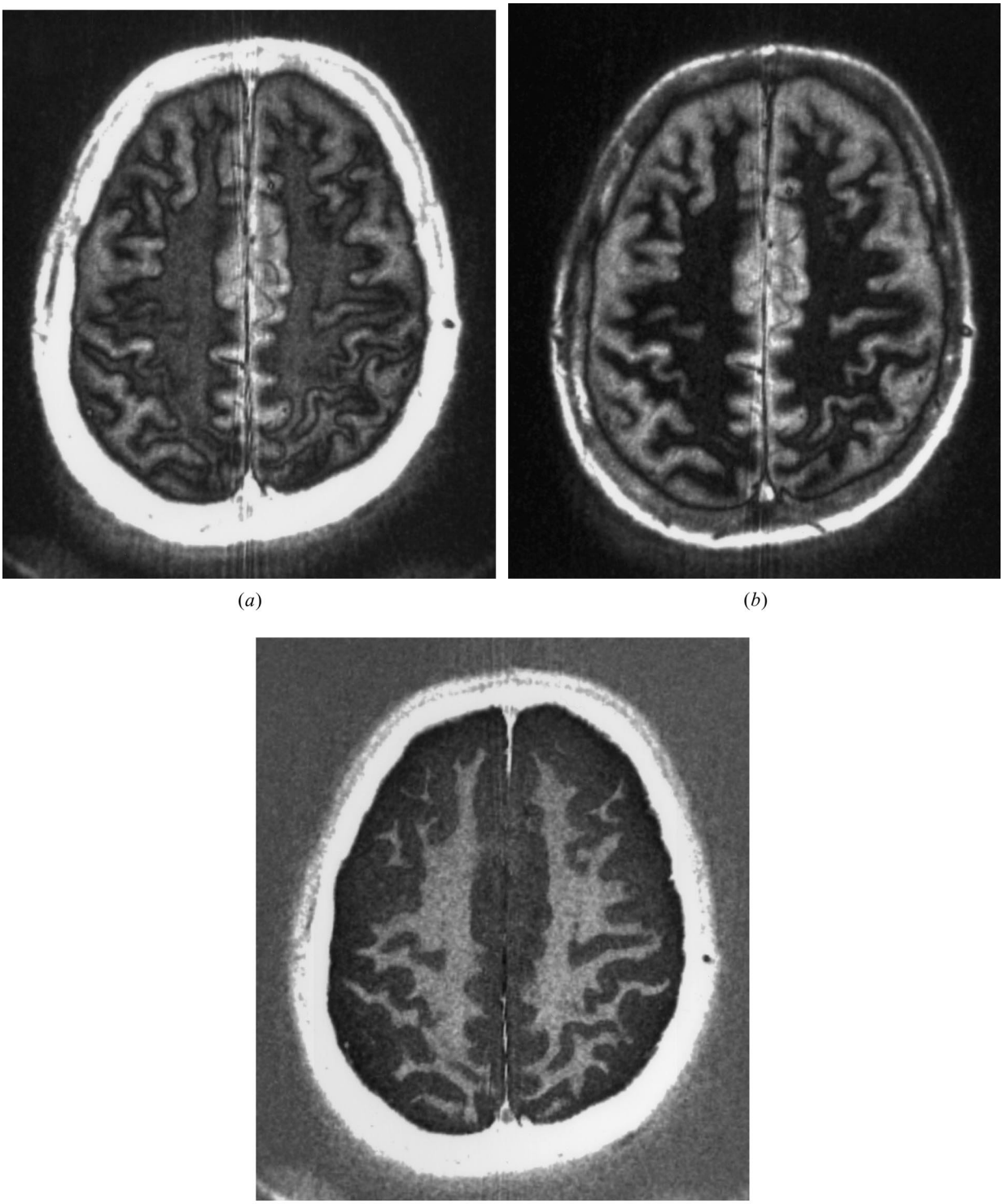

Fig. 25 – Normal brain, short T_2 components in white matter. l Stute (TR/TE/TI = 2200/0.08/360 ms, *a*), (TR/TE/TI = 2200/5.95/360 ms, *b*) and d l Stute image (*a*) minus image (*b*) to form image (*c*). Signal is seen in white matter on (*a*). It has almost disappeared at the later echo in (*b*). The difference image (*c*) formed from these two images shows the short T_2 components in white matter.

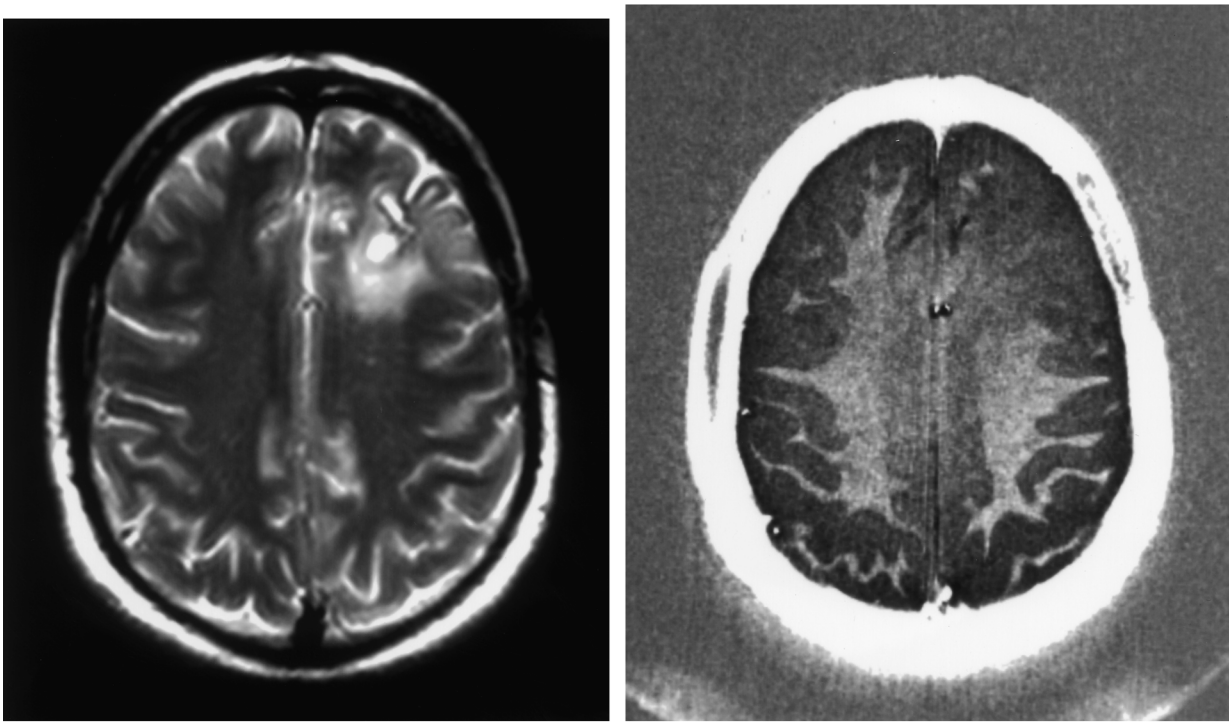

(*a*) (*b*)

Fig. 26 – Treated glioma with loss of short T_2 components in white matter. In this treated glioma SE 2500/90 (*a*) and d l Stute (TR/TE/TI = 2200/0.08/350 − 220/5.95/350 ms, *b*) images. The residual lesion after treatment with radiotherapy and chemotherapy is seen in (*a*). There is more widespread loss of signal from short T_2 components in white matter in (*b*).

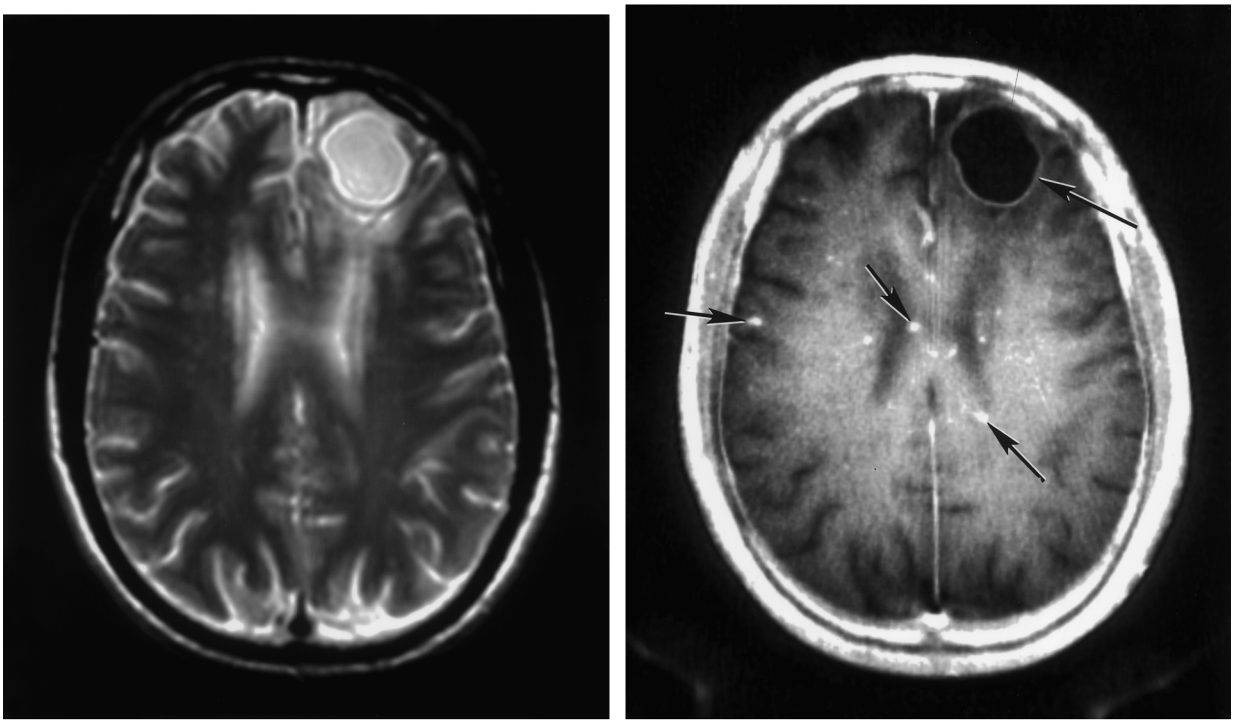

(*a*) (*b*)

Fig. 27 – Glioma after treatment and multiple angiomas. Transverse SE 2500/90 (*a*) and d Cute (TR/TE = 500/0.08 − TR/TE = 500/17.7 ms, *b*). The multiple angiomas (short arrows) are only seen on (*b*). The glioma has a high signal rim on (*b*) (long arrow) which is probably due to gliosis. It appears isointense on (*a*).

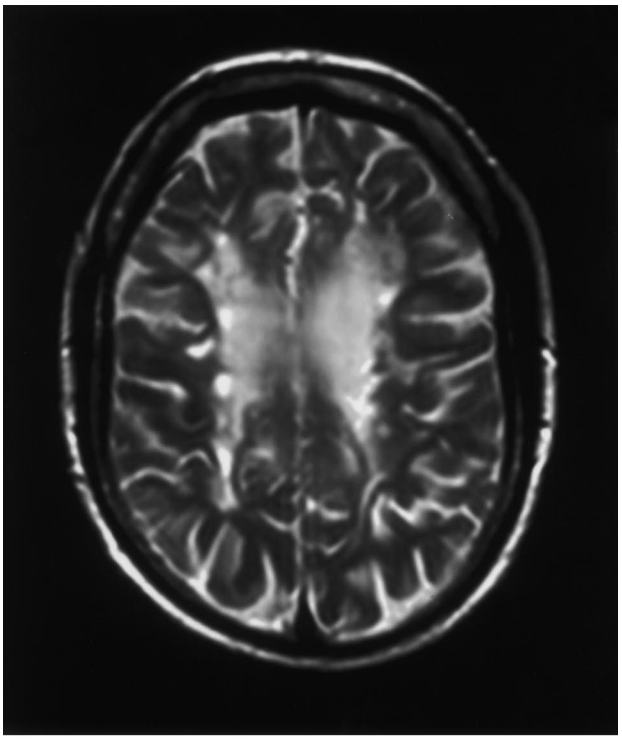

(*a*)

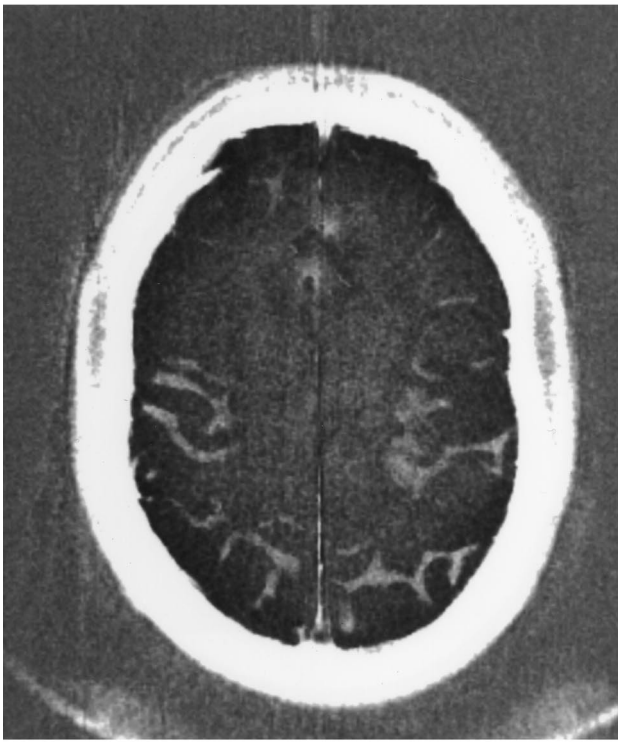

(*b*)

Fig. 28 – Multiple sclerosis with loss of short T_2 components in central white matter. Transverse SE 2500/90 (*a*) and d l Stute (TR/TE/TI = 2200/0.08/380 − 2200/5.95/380 ms, *b*). Multiple lesions are seen in (*a*). Normal short T_2 components are not apparent except in the peripheral white matter mainly in the posterior frontal and parietal lobes.

Acknowledgements. We thank the staff of the National Heart and Lung Institute, the Robert Steiner Magnetic Resonance Unit and the Department of Imaging, Hammersmith Hospitals NHS Trust including Elizabeth Burman, Angela Oatridge, Andreanna Williams, Karyn Chappell, Taigang He and Dulcie Rodrigues, as well as Diagnostic Investigations of the Spinal Conditions and Sciatica (DISCS), the Arthritis Research Council and the Golden Charitable Trust for their help.

REFERENCES

1 Henkelman RM, Stanisz GJ, Graham GJ. Magnetization transfer in MRI: a review. *NMR Biomed* 2001;14:57–64.
2 Berensden HJC. Nuclear magnetic resonance study of collagen hydration. *J Chem Phys* 1962;36:3297–3305.
3 Fullerton GD, Cameron IL, Ord VA. Orientation of tendons in the magnetic field and its effect on T_2 relaxation times. *Radiology* 1985; 155:433–435.
4 Peto S, Gillis P, Henri VP. Structure and dynamics of water in tendon from NMR relaxation measurements. *Biophys J* 1990;57:71–84.
5 Koblik PD, Freeman DM. Short echo time magnetic resonance imaging of tendon. *Invest Radiol* 1993;28:1095–1100.
6 Henkelman RM, Stanisz GJ, Kim JK, Bronskill MJ. Anisotropy of NMR properties of tissues. *Magn Reson Med* 1994; 32:592–601.
7 Hayes CW, Parellada JA. The magic angle effect in musculoskeletal MR imaging. *Top Magn Reson Imaging* 1996;8:51–56.
8 Peterfy CG, Janzen DL, Tirman PF, van Dijke CF, Pollack M, Genant HK. Magic angle phenomenon: a cause of increased signal in the normal lateral meniscus on short TE MR images of the knee. *AJR Am J Roentgenol* 1994;163:149–154.
9 Oatridge A, Herlihy AH, Thomas RW, *et al*. Magnetic resonance: magic angle imaging of the Achilles tendon. *Lancet* 2001;358: 1610–1611.
10 Marshall H, Howarth C, Larkman DJ, Herlihy AH, Oatridge A, Bydder GM. Contrast enhanced magic angle MR imaging of the Achilles tendon. *AJR Am J Roentgenol* 2002;179:192–197.
11 Schick F, Dammann K, Lutz O, Claussen CD. Adaptive techniques for clinical MR imaging of tendons. *MAGMA* 1995;3:103–107.
12 Bergin CJ, Pauly JM, Macovski A. Lung parenchyma: projection reconstruction imaging. *Radiology* 1991;179:777–781.
13 Gold GE, Pauly JM, Macovski A, Herfkens RJ. MR spectroscopic imaging of collagen: tendons and knee menisci. *Magn Reson Med* 1995; 34:647–654.
14 Schmidt MA, Yang GZ, Gatehouse PD, Firmin DN. FID-based lung MRI at 0.5 T theoretical considerations and practical implications. *Magn Reson Med* 1998;39:666–672.
15 Pauly J, Conolly S, Macovski A. Suppression of long T_2 components for short T_2 imaging. *J Magn Reson Imaging* 1992;2:145.
16 Nayak KS, Pauly JM, Gold GE, Nishimura DG. Imaging ultrashort T_2 species in the brain. *Proc Int Soc Magn Reson Med* 2000:509.
17 Bydder GM, Young IR. MR imaging: clinical use of inversion recovery pulse sequence. *J Comput Assist Tomogr* 1985;97:659–675.
18 Lu A, Grist TG, Black WF. Improved spectral selectivity and reduced susceptibility in time-FISP using a near zero TE undersampled 3D PR sequence. *Proc Int Soc Magn Reson Med* 2002:470.
19 Movin T, Kristoffersen-Wiberg M, Shalabi A, Gad A, Aspelin P, Rolf C. Intra-tendonous alterations as imaged by ultrasound and contrast medium-enhanced magnetic resonance in chronic achillodynia. *Foot Ankle Int* 1998;19:311–317.
20 Harrison R, Bronskill MJ, Henkelman RM. Magnetization transfer and T_2 relaxation components in tissue. *Magn Reson Med* 1995;33: 490–496.
21 Grenier D, Pascui O, Brighet A. Dipolar contrast for dense tissues imaging. *J Magn Reson* 2000;147:355–356.

22 Grenier D, Wachsmuth LK, Carjaval L, Majumdar S. Dipolar contrast imaging applied to *in vivo* musculo-skeletal imaging. *Proc Int Soc Magn Reson Med* 2001;9:528.
23 Navon G, Shinar H, Eliav U, Seo Y. Multiquantum filters and order in tissues. *NMR Biomed* 2001;14:112–132.
24 Ikoma K, Takamiya H, Kusaka Y, Seo Y. ^{1}H double-quantum filtered MR imaging of joint tissues: bound water specific imaging of tendons, ligaments and cartilage. *Magn Reson Imaging* 2001;19:1287–1296.
25 Brossman J, Frank LR, Pauly JM, *et al*. Short echo time projection reconstruction MR imaging of cartilage: comparison with fat suppressed spoiled GRASS and magnetization transfer contrast MR imaging. *Radiology* 1997;203:501–507.
26 Gold GE, Thedens DR, Pauly JM. MR imaging of the articular cartilage of the knee: new methods using ultrashort TEs. *AJR Am J Roentgenol* 1998;170:1223–1226.
27 Borthakur A, Reddy R, Wehrli FW. NMR studies of exchangeable hydrogen in bone. *Proc Int Soc Magn Reson Med* 1998:1804.
28 Schreiner LJ, Cameron IG, Funduk N, Miljkovic L, Pintar MM, Kydron DN. Proton NMR spin grouping and exchanged in dentin. *Biophys J* 1991;59:629–639.
29 Funduk N, Kyclon DW, Schreiner LJ, Peemoeller H, Miljkovic L, Pintar MM. Composition and relaxation of the proton magnetization of human enamel and its contribution to the tooth NMR image. *Magn Reson Med* 1984;1:66–75.
30 Sano T, Kovacs KT, Scheithauer BW, Young WF. Aging and the human pituitary gland. *Mayo Clin Proc* 1993;68:971–977.
31 Moore GR, Leung E, McKay AL *et al*. A pathology MRI study of the short T_2 component in formalin-fixed multiple sclerosis brain. *Neurology* 2000;28:1506–1510.